Sub-20 nm Si/Ge Superlattice Nanowires by Metal-Assisted Etching

Nadine Geyer,*,† Zhipeng Huang,*,†,§ Bodo Fuhrmann,‡ Silko Grimm,†
Manfred Reiche,† Trung-Kien Nguyen-Duc,† Johannes de Boor,†
Hartmut S. Leipner,‡ Peter Werner,† and Ulrich Gösele†

*Max Planck Institute of Microstructure Physics, Weinberg 2, D-06120 Halle, Germany,
Interdisciplinary Center of Materials Science, Martin Luther University
Halle-Wittenberg, Heinrich-Damerow-Strasse 4, D-01620 Halle, Germany*

ABSTRACT

An effective and low-cost method to fabricate hexagonally patterned, vertically aligned Si/Ge superlattice nanowires with diameters below 20 nm is presented. By combining the growth of Si/Ge superlattices by molecular beam epitaxy, prepatterning the substrate by anodic aluminum oxide masks, and finally metal-assisted chemical wet etching, this method generates highly ordered hexagonally patterned nanowires. This technique allows the fabrication of nanowires with a high area density of 10^{10} wires/cm^2, including the control of their diameter and length.

Arrays of semiconductor nanowires (NWs) and their heterostructures are potential candidates for applications in electronics,[1−3] optoelectronics,[4−6] and thermoelectrics[7−9] due to their unique properties such as a large surface to volume ratio as well as quantum size effects.[10,11] However, for investigating quantum effects, the dimensions of the NWs have to be comparable to the de Broglie wavelength of charge carriers, which is in the range of 10 nm. Consequently, the interest in these small NWs has increased during the last decades and a variety of fabrication strategies have been pursued. Silicon-based NWs were mainly synthesized by techniques like molecular beam epitaxy (MBE),[12−14] chemical vapor deposition (CVD),[15,16] or by laser assisted deposition (LAD) techniques.[17] These "bottom-up" approaches are based on the well-known vapor liquid solid growth concept (VLS).[18]

Additionally, alternative "top-down" approaches are under consideration with the aim to fabricate small pillars by chemical wet etching or reactive ion etching techniques. For chemical wet etching, two basic technological steps have to be solved: (i) patterning of the wafer surface with a lateral resolution of <20 nm and (ii) an anisotropic etching procedure. Imprint techniques or methods, which are based on the principles of self-assembly and self-organization,[19] are expected to solve these problems. An alternative top-

down approach combines colloidal lithography, plasma etching, and metal-assisted chemical wet etching. It represents a technique used for the fabrication of hexagonally ordered, vertically aligned Si and even Si/Ge NWs, the densities, positions, lengths, and diameters of which can be controlled.[20−23] In a former paper,[24] we presented a combination of nanosphere lithography for patterning and metal-assisted chemical wet etching. However, a series of experiments has shown that this promising technique appears to work reliably only for NWs with diameters down to 50 nm.

In this contribution, we therefore demonstrate a modified top-down approach that allows the fabrication of hexagonally well-ordered Si NWs containing a Si/Ge superlattice with diameters in the range of 10 to 20 nm. The nanospheres of the former approach were replaced by an anodic aluminum oxide (AAO) template for surface structuring. The principle of metal-assisted etching is again used to form NWs. This etching process works as a metal-induced local oxidation and dissolution of Si or Ge in a solution containing fluorine ions, where the metal acts as the catalyst.[25−28] On the basis of Si wafers containing a Si/Ge superlattice, the resulting NWs of this work are being considered as a potential structure for the production of novel light-emitting devices.[29]

We applied our technique to the formation of nanopillars in Si and Ge multilayers which were grown before by MBE on ⟨111⟩ oriented substrates. The Si/Ge multilayer structure consisted of 40 periods of alternating Si (8 ML) and Ge (2 ML) layers. This is illustrated in the transmission electron microscopy (TEM) image of Figure 1. Let us mention here that similarly sharp transitions between the Si and the Si/Ge layers cannot be achieved by VLS growth of Si/Ge hetero-

* Corresponding authors. E-mail: ngeyer@mpi-halle.mpg.de (N.G.); zhuang@mpi-halle.mpg.de (Z.H.).
† Max Planck Institute of Microstructure Physics.
‡ Interdisciplinary Center of Materials Science, Martin Luther University Halle-Wittenberg.
§ New address: Molecular Materials Research Center, Scientific Research Academy, Jiangsu University, Zhenjiang 212013, P. R. China.

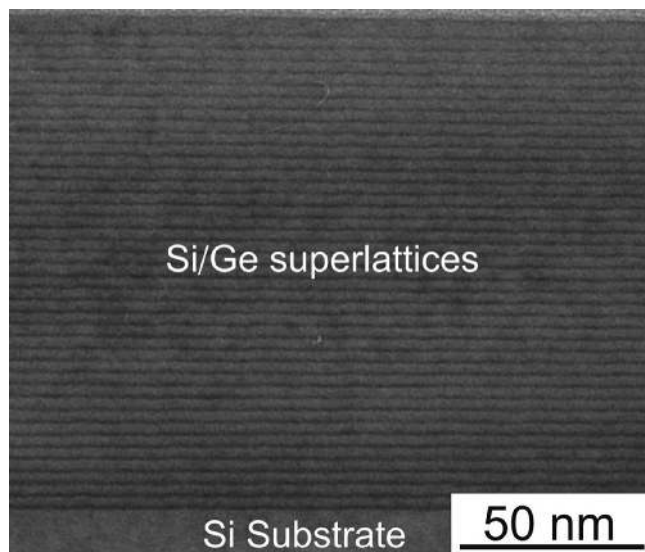**Figure 1.** TEM cross-section image of a Si/Ge superlattice structure grown by MBE. It consists of 40 periods of alternating Si (8.4 Å) and Ge (2.1 Å) layers. The period amounts to 10.5 Å.
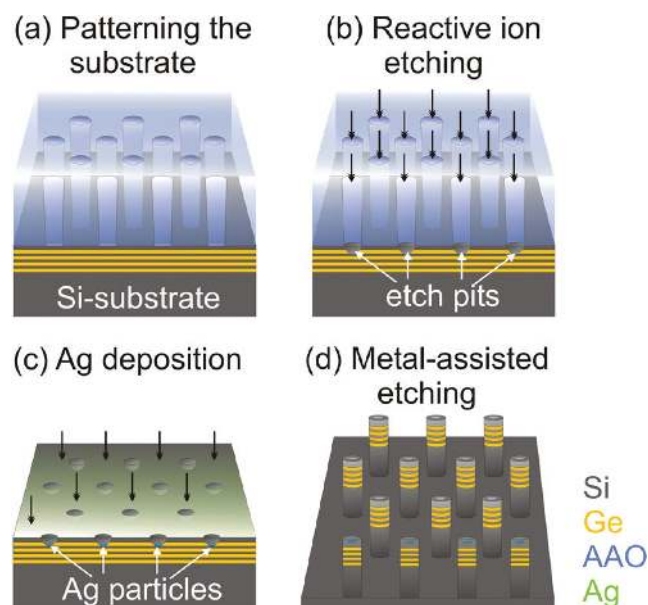

Figure 2. Schematic diagram of the fabrication technique of Si/Ge NWs by metal-assisted chemical wet etching. (a) AAO mask as a template for the Si/Ge substrate with the Si/Ge superlattice, (b) RIE through the AAO pores for etching small pits into the surface of the substrate, (c) chemical removal of the AAO mask and deposition of a thin Ag layer on the patterned substrate, (d) metal-assisted chemical wet etching using HF/H_2O_2. Finally, the Ag layer is removed and only the Si/Ge NWs remain.
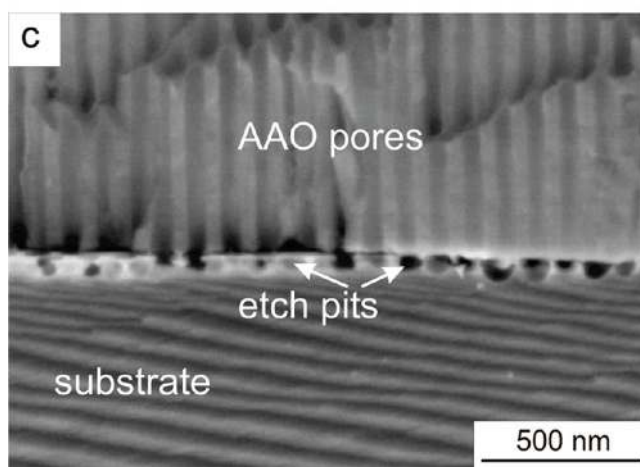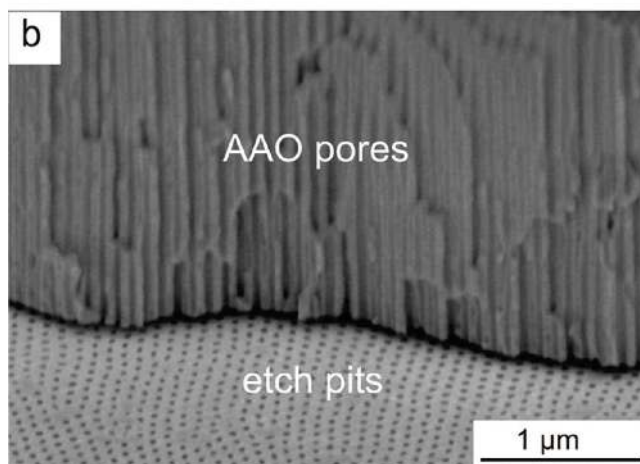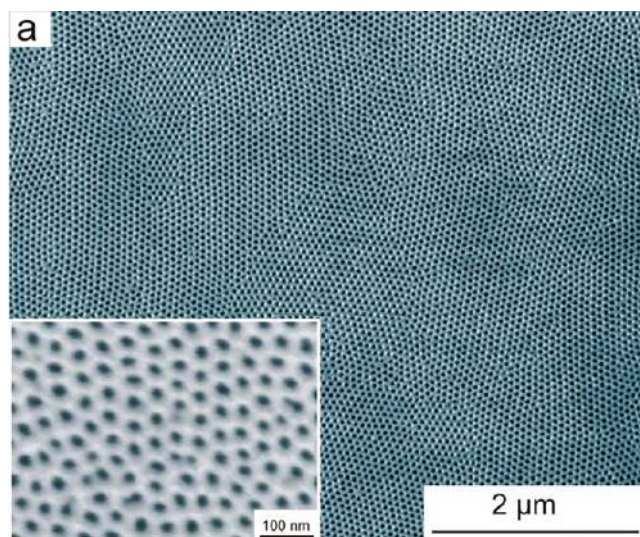

Figure 3. SEM images of the AAO templates. (a) Plan view of an AAO mask with pore diameters of 50 nm revealing the characteristic domain structure of porous AAO masks and a high magnification image of an AAO mask with pore diameters of 20 nm. (b) Tilted view of an AAO mask with 50 nm large pores on Si/Ge substrate after RIE. (c) Cross-section image of etch pits in the substrate, etched through the nanopores of the AAO template by RIE.

structures due to the about 20% solubility of Si or Ge in the catalytic Au/Si (or Au/Ge) droplet.[30]

Before starting the etching procedure, the Si substrates were cleaned by a standard RCA solution. The Si/Ge NWs were fabricated as shown in Figure 2. Self-ordered AAO masks were prepared according to techniques described in the literature.[31,32] At first, a thin Al layer of several μm was deposited on the Si/Ge substrate. The deposition was performed in a high vacuum electron beam evaporation system at a base pressure of 2×10^{-7} mbar. Second, for the

fabrication of AAO masks with pores of 20 nm diameter, the substrate was anodized in sulphuric acid. The pore diameter was determined by the choice of the acid and by
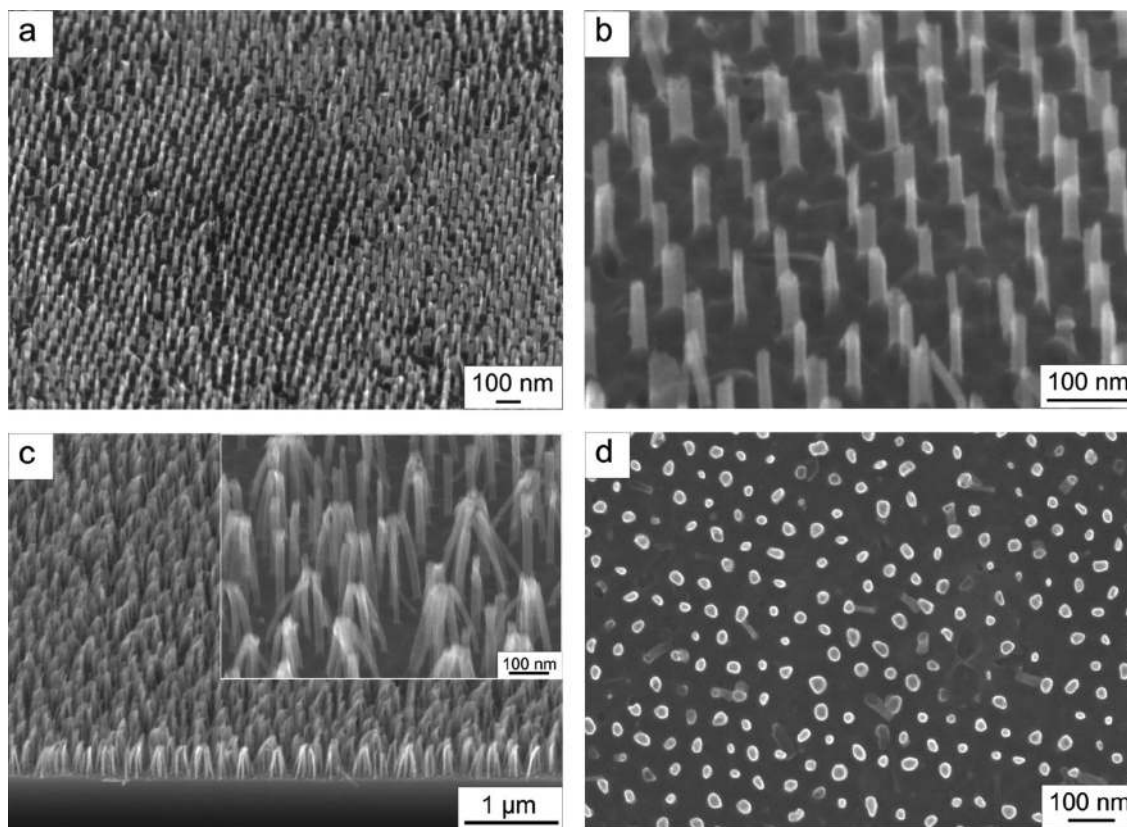
Figure 4. SEM images showing the metal-assisted etched Si/Ge NWs. (a) Large-field and (b) a detailed view of about 16 nm diameter and 100 nm long Si/Ge NWs is shown. By varying the etching time the length of the NWs is adjustable. Extending the etching time longer NWs can be obtained. In (c), a large-field image and a detailed view (inset) of Si/Ge NWs with a diameter of about 18 nm and a length of about 240 nm, and in (d), a top view of these Si/Ge NWs, is represented.

its concentration. In the case of the pores with a diameter of 50 nm, oxalic acid was used. The resulting porous AAO mask covered the whole Si/Ge substrate and acted as a template with tunable pore diameters (Figure 2a, see also Supporting Information). Third, the AAO masked substrates were treated by reactive ion etching (RIE) to form small etch pits on the surface of the substrate (Figure 2, see also Supporting Information). To remove the AAO masks, the templates were heated at 55 °C in a phosphoric acid (85 wt %) bath diluted with H_2O in the ratio of 1:3 for a duration of 20 min. Subsequently, an Ag film with a thickness of 15 nm was sputtered onto the patterned substrate. The Ag film covered the whole substrate except for the sidewalls of the etch pits (Figure 2c). The bottom of the etch pits was also covered by Ag particles. The experiments showed that substantial etching of the Si/Ge substrate only occurs at regions that are covered by a thin Ag layer. No remarkable etching could be observed in the etch pits. A catalytic effect of small Ag particles at the bottom of the etch pits seems to be negligible as had also been demonstrated for the case of Si NWs.[33] After the Ag deposition, the Ag structured substrates were etched in darkness in an etching mixture consisting of 4.6 M HF and 0.44 M H_2O_2 at room temperature for 10 s. As a result of etching, an ordered array of Si/Ge NWs was formed. As a final step, the Ag layer was removed by aqua regia and only the Si/Ge NWs remained (Figure 2d).

In Figure 3a, a scanning electron microscopy (SEM) plan view of the AAO mask with open pores is shown. The diameters of the pores used in this particular experiments range from 20 to 50 nm. A domain structure is visible. Within a single domain, the pores exhibit a hexagonal arrangement. Because of the domain formation of the pores in the AAO mask the resulting Si/Ge NWs were also arranged in domains. The AAO mask was partially removed in the foreground of Figure 3b, and the small etch pits produced by RIE become visible. Their diameters correspond to the diameter of the parent AAO pores. The in-plan width, the depth, and the shape of the etch pits can be adjusted by varying the RIE parameters. Figure 3c represents a SEM cross-section image of the etch pits with a depth of about 50 nm on top of the multilayer.

The thickness of the Ag film sputtered after removal of the AAO mask is a critical parameter and has to be optimized for each individual structure. Our experiments showed that for an Ag film with a thickness below 15 nm the fabrication of Si/Ge NWs failed. In this case, the Ag film was characterized by small islands of isolated Ag particles. For a film with thickness above 15 nm, the Ag film formed a network of connected Ag islands with small pores inside.[34] This network structure of the Ag layer was essential for the controlled formation of NWs. Using this method, the fabrication of extended arrays of Si/Ge NWs with a smooth surface and a high area density of 10^{10} wires/cm^2 was
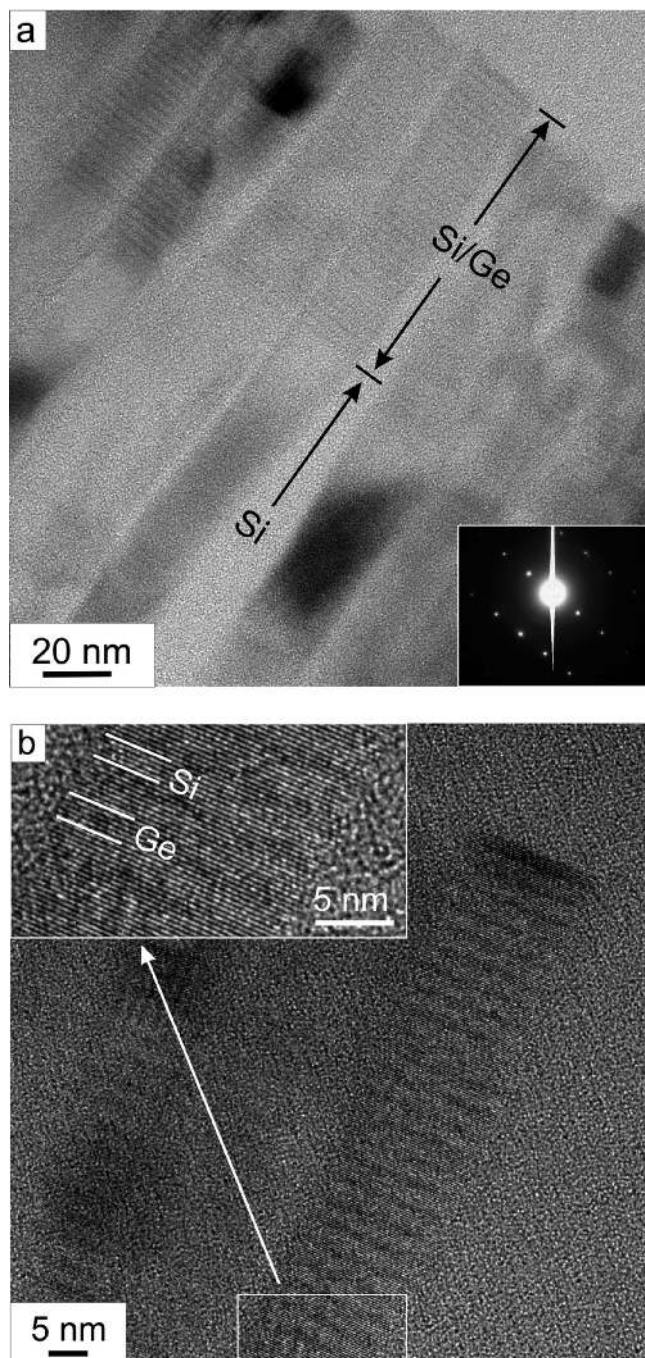
Figure 5. Structure of the fabricated Si/Ge NWs. (a) TEM image indicates clearly the Si and Ge heterostructures of the 18 nm diameter Si/Ge NWs. Sharp transitions between the Si and the Si/Ge layers are visible. The inset is the selected area electron diffraction image showing the single crystallinity of the Si/Ge NWs. (b) High-resolution TEM cross-sectional image of two NWs. The magnified TEM lattice image in the inset demonstrates the single crystallinity of the Si/Ge NWs.

accomplished. In the case of AAO masks with a pore diameter of 20 nm, the average diameter of the Si/Ge NWs was (16.1 ± 4.6) nm.

A representative large-field image and detailed view of about 16 nm thick vertically aligned Si/Ge NWs are shown in Figure 4a and 4b. These nanowires have lengths of about 100 nm. By extending the etching time, Si/Ge superlattice nanowires with higher aspect ratio features can be produced.

In the large-field image of Figure 4c, extended areas of well-ordered nanowires with a common length of about 240 nm and an average diameter of about 18 nm are illustrated. Because of surface tension force exerted on the NWs during drying of the sample and a large aspect ratio of about 13, the tips of the NWs stick together as can be seen in the inset of Figure 4c.

The shapes of the resultant Si/Ge superlattice nanowires conform in general to the shape of the pores in the parent AAO mask. As shown in Figure 2a above, the geometry of the pores of the AAO template is not perfectly round, which reflects the shape of the corresponding NWs as can be seen in a top view of NWs in Figure 4d.

The NWs containing a Si/Ge superlattice were characterized by TEM. Figure 5a represents a micrograph of highly crystalline NWs with 18 nm diameter and a length of about 240 nm.. The superlattice inside the metal-assisted etched NWs is clearly visible. Additionally, a high resolution (HRTEM) image in Figure 5b proves the crystallinity of these NWs.

In conclusion, we demonstrated that the combination of the growth of Si/Ge superlattices by MBE, surface prepatterning by AAO templates, and metal-assisted wet chemical etching can be successfully applied to fabricate NWs containing a Si/Ge superlattice. Using this method, we obtained highly crystalline Si/Ge NWs with a diameter below 20 nm. The diameter can be controlled via the pore diameter of the AAO template. An aspect ratio of over 10 and a high area density of 10^{10} wires/cm^2 can be achieved. This method allows a novel standard in the fabrication of complex NWs, which are considered to be promising structures for the fabrication of light-emitting diodes.

Supporting Information Available: Experimental details about the fabrication of anodic aluminum oxide templates and about the RIE procedure. This material is available free of charge via the Internet at http://pubs.acs.org.

References
(1) Goldberger, J.; Hochbaum, A. I.; Fan, R.; Yang, P. *Nano Lett.* **2006**, *6*, 973.
(2) Schmidt, V.; Riel, H.; Senz, S.; Karg, S.; Riess, W.; Gösele, U. *Small* **2005**, *2*, 85.
(3) Huang, Y.; Lieber, C. M. *Pure Appl. Chem.* **2004**, *76*, 2051.
(4) Agarwal, R.; Lieber, C. M. *Appl. Phys. A: Mater. Sci. Proc.* **2006**, *85*, 209.
(5) Cui, Y.; Lieber, C. M. *Science* **2001**, 851.
(6) Peng, K. Q.; Xu, Y.; Wu, Y.; Yan, Y. J.; Lee, S. T.; Zhu, J. *Small* **2005**, *1*, 1062.
(7) Hochbaum, A. I.; Chen, R.; Delgado, R. D.; Liang, W.; Garnett, E. C.; Najarian, M.; Majumdar, A.; Yang, P. *Nature* **2008**, *451*, 163.
(8) Hicks, L. D.; Dresselhaus, M. S. *Phys. Rev. B* **1993**, *47*, 16631.
(9) Boukai, A.; Bunimovich, Y.; Tahir-Kheli, J.; Yu, J.-K.; Goddard, W. A.; Heath, J. *Nature* **2008**, *451*, 168.
(10) Usami, N.; Mine, S.; Fukatsu, S.; Shiraki, Y. *Appl. Phys. Lett.* **1994**, *64*, 1126.
(11) Lieber, C. M. *MRS Bull.* **2003**, *28*, 128.
(12) Schubert, L.; Werner, P.; Zakharov, N. D.; Gerth, G.; Kolb, F.; Long, L.; Gösele, U.; Tan, T. Y. *Appl. Phys. Lett.* **2004**, *84*, 4968.
(13) Werner, P.; Zakharov, N. D.; Gerth, G.; Schubert, L.; Gösele, U. *Int. J. Mater. Res.* **2006**, *97*, 1008.

(14) Fuhrmann, B.; Leipner, H. S.; Höche, H.-R.; Schubert, L.; Werner, P.; Gösele, U. *Nano Lett.* **2005**, *5*, 2524.

(15) Cui, Y.; Lauhorn, L. J.; Gudiksen, M.; Wang, J.; Lieber, C. M. *Appl. Phys. Lett.* **2001**, *78*, 2214.

(16) Westwater, J.; Gosain, D. P.; Usui, S. *Phys. Stat. Solidi A* **1998**, *165*, 37.

(17) Yang, Y.-H.; Wu, S.-J.; Chiu, H.-S.; Lin, P.-I.; Chen, Y.-T. *J. Phys. Chem. B* **2004**, *108*, 846.

(18) Wagner, R. S.; Ellis, W. C. *Appl. Phys. Lett.* **1964**, *4*, 89.

(19) Sinitski, A.; Neumeier, S.; Nelles, J.; Fischler, M.; Simon, U. *Nanotechnology* **2007**, *18*, 305307.

(20) Hulteen, J. C.; Treichel, D. A.; Smith, M. T.; Duval, M. L.; Jensen, T. R.; Van Duyne, R. P. *J. Phys. Chem. B* **1999**, *103*, 3854.

(21) Cheung, C. L.; Nikolic', R. J.; Reinhardt, C. E.; Wang, T. F. *Nanotechnology* **2006**, *17*, 1339.

(22) Peng, K.; Zhang, M.; Lu, A.; Wong, N.; Zhang, R.; Lee, S. *Appl. Phys. Lett.* **2007**, *90*, 163123.

(23) Wang, X.; Pey, K. L.; Choi, W. K.; Ho, C. K. F. *Electrochem. Solid-State Lett.* **2009**, *12*, 37.

(24) Huang, Z. P.; Fang, H.; Zhu, J. *Adv. Mater.* **2007**, *19*, 744.

(25) Li, X.; Bohn, P. W. *Appl. Phys. Lett.* **2000**, *77*, 2572.

(26) Douani, R.; Si-Larbi, K.; Hadjersi, T.; Megouda, N.; Manseri, A. *Phys. Status Solidi A* **2007**, *205*, 225.

(27) Chartier, C.; Bastide, S.; Lévy-Clément, C. *Electrochim. Acta* **2008**, *53*, 5509.

(28) Huang, Z.; Shimizu, T.; Senz, S.; Zhang, Z.; Zhang, X.; Lee, W.; Geyer, N.; Gösele, U. *Nano Lett.* **2009**, *9*, 2519.

(29) Talalaev, V. G.; Cirlin, G. E.; Tonkikh, A. A.; Zakharov, N. D.; Werner, P.; Gösele, U.; Tomm, J. W.; Elsaesser, T. *Nanoscale Res. Lett.* **2006**, 137.

(30) Clark, T. E.; Nimmatoori, P.; Lew, K.-K.; Pan, L.; Redwing, J. M.; Dickey, E. C. *Nano Lett.* **2008**, *8*, 1246.

(31) Masuda, H.; Fukuda, K. *Science* **1995**, *268*, 1466.

(32) Jessensky, O.; Müller, F.; Gösele, U. *J. Electrochem. Soc.* **1998**, *145*, 3735.

(33) Huang, Z.; Zhang, X.; Reiche, M.; Liu, L.; Lee, W.; Shimizu, T.; Senz, S.; Gösele, U. *Nano Lett.* **2008**, *8*, 3046.

(34) Fang, H.; Wu, Y.; Zhao, J.; Zhu, J. *Nanotechnology* **2006**, *17*, 3768.

NL900751G